Scientific Research Publishing

Journal of Biosciences and Medicines, 2024, 12, 251-265
https://www.scirp.org/journal/jbm
ISSN Online: 2327-509X
ISSN Print: 2327-5081

Quasi-Static, Poiseuille Flow of Analgesics from an Elastomeric Pump: Theoretical Determination of Infusion Times and Toxicity Conditions

Clare B. Lipscombe[1], Trevor C. Lipscombe[2], Don S. Lemons[3]

[1]Division of General Surgery, Vanderbilt University Medical Center, Nashville, TN, USA
[2]Catholic University of America Press, Washington DC, USA
[3]Department of Physics, Bethel College, North Newton, KS, USA
Email: Clare.lipscombe@vumc.org, lipscombe@cua.edu, lemons.don@gmail.com

How to cite this paper: Lipscombe, C.B., Lipscombe, T.C. and Lemons, D.S. (2024) Quasi-Static, Poiseuille Flow of Analgesics from an Elastomeric Pump: Theoretical Determination of Infusion Times and Toxicity Conditions. *Journal of Biosciences and Medicines*, **12**, 251-265.
https://doi.org/10.4236/jbm.2024.129023

Received: August 25, 2024
Accepted: September 23, 2024
Published: September 26, 2024

Abstract

Background: Elastomeric pumps (elastic balls into which analgesics or antibiotics can be inserted) push medicines through a catheter to a nerve or blood vessel. Since elastomeric pumps are small and need no power source, they fit easily into a pocket during infusion, allowing patient mobility. Elastomeric pumps are widely used and widely studied experimentally, but they have well-known problems, such as maintaining reliable flow rates and avoiding toxicity or other peak-and-trough effects. **Objectives:** Our research objective is to develop a realistic theoretical model of an elastomeric pump, analyze its flow rates, determine its toxicity conditions, and otherwise improve its operation. We believe this is the first such theoretical model of an elastomeric pump consisting of an elastic, medicine-filled ball attached to a horizontal catheter. **Method:** Our method is to model the system as a quasi-Poiseuille flow driven by the pressure drop generated by the elastic sphere. We construct an engineering model of the pressure exerted by an elastic sphere and match it to a solution of the one-dimensional radial Navier-Stokes equation that describes flow through a horizontal, cylindrical tube. **Results:** Our results are that the model accurately reproduces flow rates obtained in clinical studies. We also discover that the flow rate has an unavoidable maximum, which we call the "toxicity bump", when the radius of the sphere approaches its terminal, unstretched value—an effect that has been observed experimentally. **Conclusions:** We conclude that by choosing the properties of an elastomeric pump, the toxicity bump can be restricted to less than 10% of the earlier, relatively constant flow rate. Our model also produces a relation between the length of

time that the analgesic fluid infuses and the physical properties of the fluid, of the elastomeric sphere and the tube, and of the blood vessel into which the analgesic infuses. From these, we conclude that elastomeric pumps can be designed, using our simple model, to control infusion times while avoiding toxicity effects.

Keywords

Elastomeric Pump, Infusion Therapy, Bio-Fluids, Medical Devices, Antibiotic Delivery, Analgesic Delivery

1. Introduction

Background

The rate of infusion is a critical component of optimizing the delivery of analgesics and other medications. In emergency trauma situations, priority is placed on delivering therapeutic agents as fast as possible. Common field techniques in critical situations even include such measures as manually squeezing infusion bags, inflating blood pressure cuffs around bags, and kneeling on bags to achieve a rapid rate of transfusion of IV fluids to a crashing hypotensive patient. In patients with critical blood loss, rapid transfusers are often used to administer blood products for immediate resuscitation.

And yet, other situations call for tight regulation of flow rates. When administering drugs with greater levels of toxicity, such as analgesics, chemotherapeutic agents, and antibiotics, controlling the infusion rate becomes essential. As such, elastomeric pumps provide caretakers and patients with a reliable, mobile infusion system that can be used for patients receiving intravenous chemotherapy, antibiotics, and post-operative analgesia.

For example, vancomycin remains one of the most powerful antibiotics available due to its strong efficacy against beta-lactam-resistant, gram-positive organisms [1]. However, its dosing must be closely titrated based on patients' serum levels and renal function because of its renal toxicity. For this reason, not only is it important to maintain a steady concentration of vancomycin, but the infusion rate must also be closely controlled to avoid the development of red man syndrome, a severe reaction characterized by a diffuse, pruritic rash with possible fever, hypotension, and angioedema secondary to the widespread release of histamine [2]. Most protocols require vancomycin to be administered over the course of a 60-minute interval. However, studies have also determined that smaller, more frequent doses of vancomycin are the optimal infusion technique. Because elastomeric pumps can infuse over a period of hours to days, and their single-use disposability makes it convenient for frequent administration, even for patients at home, this technology proves advantageous for antibiotic delivery. This is also true for analgesic and chemotherapeutic agents, as most of these drugs have the potential to cause infusion reactions.

Methods

We model an elastomeric pump as an elastic sphere that is filled beyond its unstretched radius with a viscous fluid under pressure. The stretched elastomer exerts pressure on the antibiotic or analgesic fluid, which flows out of the sphere through hollow tubing, which we model as a horizontal, hollow cylinder of uniform diameter. Under the usual conditions, the flow is axially symmetric, steady state, and Poiseuille. Thus, we are able to describe these flows with scaling laws and analytic expressions that can be solved numerically with commercially available software packages. These solutions could be used to design and optimize elastomeric pumps.

Significance

Elastomeric pumps have considerable advantages in terms of quality of life. For these systems do not rely on battery or electrical power, so that patients have a great deal of flexibility while receiving treatment. Instead of being restricted to an IV pole, patients are free to move. This provides hospital patients the opportunity to be more active and participate in physical therapy, which is important for post-operative patients and their long-term outcomes. For patients using these pumps in the outpatient setting, it allows their treatments to not interfere with their activities of daily living. The portability and safety of these devices allow patients to receive reliable and efficacious treatment at home instead of occupying hospital beds [3] [4].

The relatively new use of these devices in delivering localized analgesia could be a substantial development in post-operative pain control. Although this delivery method for pain control provides substantial benefits over systemic analgesia, studies have shown that the actual flow rates produced by elastomeric pumps have a statistically significant difference from their manufacturer-set flow rates in up to 47% of pumps, depending on the manufacturer [5]. This limits the versatility of elastomeric pumps as low flow rates will be inadequate to provide pain relief and high flow rates could result in serious side effects—including central nervous system dysfunction, autonomic dysfunction, and even cardiovascular toxicity. As a corrective, the model we develop here allows the operation of elastomeric pumps to be precisely and reliably optimized. In this way, elastomeric pumps could offer a safe alternative to commonly used methods for delivering opioid medications and pain control regimes that carry a high risk of developing unwanted dependence [6].

Organization

This paper is organized as follows. Section 1 "Introduction" expands on the background and significance of our work. Sections 2 - 5 develop, in logical sequence, our theoretical model of an elastomeric pump. First, in Section 2, we describe Poiseuille flow in the catheter tube as driven by a pressure gradient that changes slowly in time. A. N. Gent's equation of state of an elastic sphere [7] (§3.2), presented in Section 3, determines the pressure exerted on the fluid. Together, these two sections (2 and 3) construct the two parts of our model, pump bulb and

catheter tube. We join these two parts in Section 4 and, in this way, determine the infusion flow rate produced by the pump. Section 5 allows us to numerically solve for the radius of the elastomeric sphere and the flow rate in the tube as a function of time. In Section 6, we make explicit the conditions under which quasi-static, Poiseuille flow obtains. In Section 7, we present extensions of the model that account for power-law, non-Newtonian fluids, and the flow of a Newtonian fluid at higher Reynolds numbers by means of a Darcy-Weisbach equation with a Blasius friction factor. In Section 8, we discuss our results. Section 9 concludes.

2. Navier-Stokes Equation and Quasi-Static Poiseuille Flow

Consider the flow of a Newtonian fluid through a horizontal tube of length L and radius R, driven by a pressure drop ΔP. The dynamics of the fluid in the cylindrical tube is governed by the one-dimensional, incompressible, Navier-Stokes equation [8]:

$$\rho\frac{\partial u}{\partial t}=\frac{\mu}{r}\frac{\partial}{\partial r}\left(r\frac{\partial u}{\partial r}\right)+\frac{\Delta P}{L} \tag{1}$$

where, $u\left[=u\left(r,t\right)\right]$ is the axially directed, time-dependent fluid velocity in a cylindrically symmetric channel at a radius r, μ is the viscosity of the fluid, and ρ is its density [9].

The time-independent solution to (1) solves:

$$0=\frac{\mu}{r}\frac{\mathrm{d}}{\mathrm{d}r}\left(r\frac{\mathrm{d}u}{\mathrm{d}r}\right)+\frac{\Delta P}{L} \tag{2}$$

when the pressure drop ΔP is constant in time. The velocity profile $u\left(r\right)$ that solves (2), called Poiseuille flow, is given by:

$$u\left(r\right)=\frac{\Delta P}{4\mu L}\left(R^2-r^2\right) \tag{3}$$

The average flow rate $\bar{u}$. is found by integrating (3) over a tube cross-section of radius R. In this way, we find that $\bar{u}=R^2\Delta P/8\mu L$. Consequently, the time-independent, average volumetric flow rate or flux $Q=\pi R^2\bar{u}$ is given by:

$$Q=\frac{\pi R^4}{8\mu L}\Delta P \tag{4}$$

The flux Q remains directly proportional to the pressure gradient even when the tubing has a non-circular cross-section [10].

Even when the pressure gradient ΔP varies slowly with time, Equation (4) is maintained, as time-dependent, quasi-static, Poiseuille flow is established [11]. Then, the flux is described by:

$$Q\left(t\right)=\frac{\pi R^4}{8\mu L}\Delta P\left(t\right) \tag{5}$$

where these time dependencies are slow. We will examine the conditions under which quasi-static, Poiseuille flow is maintained in Section 6.

The pressure difference ΔP between the fluid in the elastic sphere and the blood in a vessel (or "vein") is given by $\Delta P = P_{fluid} - P_{vein}$. Hence, the volumetric flow rate Q from the sphere to the vein is governed by:

$$Q = \frac{\pi R^4}{8\mu L}\left(P_{fluid} - P_{vein}\right) \tag{6}$$

The pressure of the fluid in the elastic sphere P_{fluid} and the pressure in the blood vessel P_{vein} are each composed of two parts. The pressure on the fluid is that exerted by the elastic sphere P_{elast} plus that exerted by the atmosphere P_{atmos}, so that:

$$P_{fluid} = P_{elast} + P_{atmos}, \tag{7}$$

and the pressure exerted by the blood in the vessel is:

$$P_{vein} = P_{sphyg} + P_{atmos} \tag{8}$$

where P_{sphyg} is the pressure measured by a sphygmomanometer or blood-pressure cuff. Thus, the volume fluid flow rate (6) is expressed by:

$$Q = \frac{\pi R^4}{8\mu L}\left(P_{elast} - P_{sphyg}\right), \tag{9}$$

where the pressure P_{sphyg} is directly measured in a clinical setting, the pressure P_{elast} must be inferred from a model of the pump's elastic sphere.

3. Pressure Exerted by an Elastic Sphere

The pressure P_{elast} exerted by the elastic sphere of an elastomeric pump on the fluid it contains is a function of the sphere's material properties and, of course, the sphere's size compared to that when unstretched. For this functionality, we adopt the equation of state devised by the late material scientist and rubber engineer A. N. Gent [7] (§2.3).

Gent expressed his equations of state in terms of a "stretch ratio" λ, defined as the ratio of the instantaneous radius of the sphere r to its relaxed or unstretched radius $r_{\min}$, so that $\lambda = r/r_{\min}$ $\left[\geq 1\right]$. For a thin-walled, isotropic, elastomeric sphere,

$$P_{elast} = \left(\frac{w}{r_{\min}}\right)\frac{2}{\lambda^3}t, \tag{10}$$

where w is the width or thickness of the unstretched wall material and t is the isotropic tangential stress exerted by the sphere. The tangential stress t, in turn, is related to the stress ratio λ of an elastic sphere by:

$$t = \frac{E\lambda^2}{3}\left(1 - \frac{1}{\lambda^6}\right)\left(\frac{1}{1 - \frac{J(\lambda)}{J_{\max}}}\right) \tag{11}$$

where

$$J(\lambda) = 2\lambda^2 + \frac{1}{\lambda^4} - 3, \tag{12}$$

$J_{\max} = J(\lambda_{\max})$, with $\lambda_{\max}$ the maximum allowed stretch ratio, and E is the elastic (or Young's) modulus of the material composing the elastic sphere.

Given (10) and (11), we find that:

$$P_{elast} = \left(\frac{2}{3}\right)\left(\frac{wE}{r_{\min}}\right)\left(\frac{1}{\lambda}\right)\left(1-\frac{1}{\lambda^6}\right)\left(\frac{1}{1-\dfrac{J(\lambda)}{J_{\max}}}\right). \tag{13}$$

When the right-hand side of (13) is normalized,

$$\frac{r_{\min}}{wE}P_{elast} = \frac{2}{3}\left(\frac{1}{\lambda}\right)\left(1-\frac{1}{\lambda^6}\right)\left(\frac{1}{1-\dfrac{J(\lambda)}{J_{\max}}}\right). \tag{14}$$

The first factor in parentheses $(1/\lambda)$ on the right-hand side of (14) is the usual Young-Laplace factor. The second is Merritt and Weinhaus's correction [12] that requires the pressure exerted by the elastic sphere to vanish when the sphere is completely relaxed, that is, when $\lambda = 1$. The third factor is Gent's contribution, which incorporates the effect of the elastic sphere approaching its elastic limit. After all, the material will not stretch indefinitely. Rather, the elastomer will rupture before reaching its maximum stretch ratio $\lambda_{\max}$.

According to Gent, the Young's modulus of the material E is proportional to the "number of molecular strands in the network per unit volume". Thus, identically sized elastic spheres composed of different materials will have different Young's moduli E and different maximum stretch ratios $\lambda_{\max}$. Different elastomer values of E and $\lambda_{\max}$ will cause different pressures to be exerted on the fluid within the sphere and lead to different flow rates, a phenomenon observed in experiments comparing silicone and polyisoprene diffusers [13].

4. Flow Rate in an Elastomeric Pump

The volumetric flow rate Q caused by the pressure exerted by the elastic sphere of an elastomeric pump is, according to (9) and (13), given by:

$$Q(\lambda) = \frac{\pi R^4}{8\mu L}\left[\frac{2wE}{3r_{\min}}\left(\frac{1}{\lambda}\right)\left(1-\frac{1}{\lambda^6}\right)\left(\frac{1}{1-\dfrac{J(\lambda)}{J_{\max}}}\right) - P_{sphyg}\right]. \tag{15}$$

We rewrite this as:

$$\tilde{Q}(\lambda) = \frac{1}{\lambda}\left(1-\frac{1}{\lambda^6}\right)\left(\frac{1}{1-\dfrac{J(\lambda)}{J_{\max}}}\right) - \tilde{P}_{sphyg} \tag{16}$$

where we have introduced the dimensionless parameters:

$$\tilde{Q} = \frac{12 r_{\min} \mu L}{\pi w E R^4} Q \tag{17}$$

and

$$\tilde{P}_{sphyg} = \frac{3 r_{\min}}{2 w E} P_{sphyg} . \tag{18}$$

Recall from (12) that $J(\lambda) = 2\lambda^2 + \lambda^{-4} - 3$.

If the catheter is inserted into a blood vessel where the blood pressure is relatively low, then flow is from the sphere to the catheter. This is the usual case. If, however, the catheter is inserted into a vessel at higher pressure, then the flow will be from the catheter to the sphere, whose radius $r(t)$ will increase. This describes the blood-donation process.

Figure 1 shows a normalized, volumetric, flow rate $\tilde{Q}$ with $\lambda_{\max} = 4$ and $\tilde{P}_{sphyg} = 0.1$. In general, $\tilde{P}_{sphyg}$ is small compared to the other terms in (16) and simply subtracts a small constant amount from its right-hand side. We can replicate laboratory investigations in which fluid flows from the pump through the tubing and into an open container by setting $\tilde{P}_{sphyg} = 0$ in (16). See References [5] and [13].

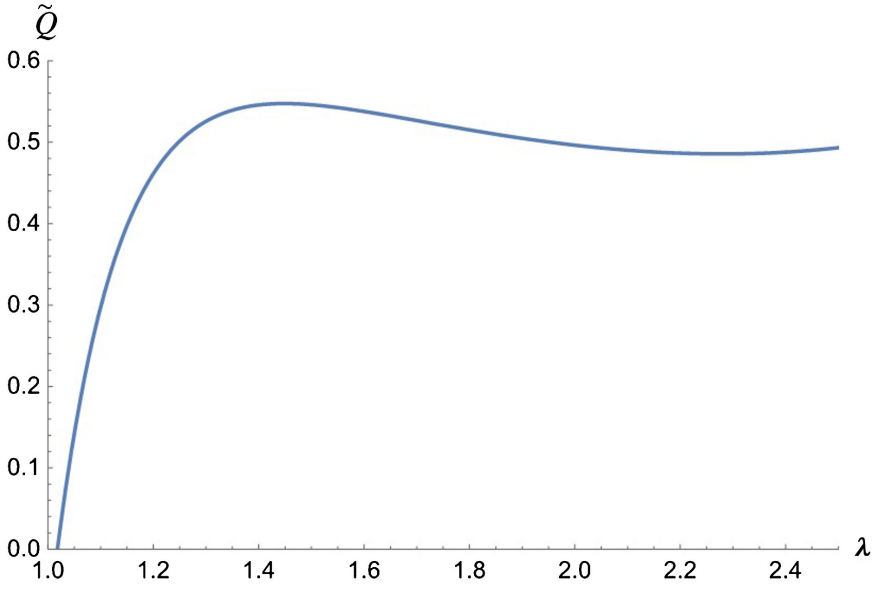

Figure 1. Normalized, volumetric, flow rate $\tilde{Q}$ versus stretch ratio λ from Equation (16) with $\tilde{P}_{sphyg} = 0.1$ and $\lambda_{\max} = 4$. The toxicity bump occurs at a peak stretch ratio λ_{peak} close to $7^{1/6} \approx 1.38$ when $\lambda_{\max} \gg \lambda_{peak} > 1$.

Equation (16) leads to a toxicity effect, shown in **Figure 1** as a bump in the flow rate, which we obtain by numerically finding the stretch ratio λ_{peak} that maximizes $\tilde{Q}(\lambda)$ as a function of λ. When the maximum stretch ratio $\lambda_{\max} \gg \lambda_{peak}$, the toxicity bump can be found by maximizing $\lambda^{-1}(1-\lambda^{-6})$. Thus,

$$\lambda_{peak} = 7^{1/6} \approx 1.38 \tag{19}$$

and $\left(\frac{1}{7^{1/6}}\right)\left(1-\frac{1}{7}\right)-\tilde{P}_{sphyg}\approx 0.52$ when $\tilde{P}_{sphyg}=0.1$. Indeed, the peak normalized flow rate in Figure 1 appears to be approximately 0.54.

5. Infusion Time

The instantaneous volume flux $Q(t)$ is related to the instantaneous radius $r(t)$ of the elastic sphere as a function of time t through the equation:

$$Q=-4\pi r^2\frac{\mathrm{d}r}{\mathrm{d}t}. \tag{20}$$

Given (20) and (15),

$$-4\pi r^2\frac{\mathrm{d}r}{\mathrm{d}t}=\frac{\pi R^4}{8\mu L}\left[\frac{2wE}{3r_{\min}}\left(\frac{1}{\lambda}\right)\left(1-\frac{1}{\lambda^6}\right)\left(\frac{1}{1-\frac{J(\lambda)}{J_{\max}}}\right)-P_{sphyg}\right] \tag{21}$$

or

$$\frac{48r_{\min}^4\mu L}{wER^4}\lambda^2\frac{\mathrm{d}\lambda}{\mathrm{d}t}=\left[\tilde{P}_{sphyg}-\left(\frac{1}{\lambda}\right)\left(1-\frac{1}{\lambda^6}\right)\left(\frac{1}{1-\frac{J(\lambda)}{J_{\max}}}\right)\right], \tag{22}$$

that is,

$$\lambda^2\frac{\mathrm{d}\lambda}{\mathrm{d}\tau}=\left[\tilde{P}_{sphyg}-\left(\frac{1}{\lambda}\right)\left(1-\frac{1}{\lambda^6}\right)\left(\frac{1}{1-\frac{J(\lambda)}{J_{\max}}}\right)\right] \tag{23}$$

where we have introduced the dimensionless time:

$$\tau=\frac{wER^4}{48r_{\min}^4\mu L}t. \tag{24}$$

The ratio $48r_{\min}^4\mu L/wER^4$ is a characteristic time that governs the infusion dynamics. Recall that w is the unstretched width or thickness of the sphere material, E is its Young's modulus, R is the radius of the tubing to which the elastomeric pump is attached, $r_{\min}$ is the unstretched radius of the elastomeric pump sphere, μ is the fluid viscosity, and L is the tube length. Thus, the more viscous the antibiotic and the longer and thinner the tube, the more time the infusion requires. And the stiffer the elastomer and the thicker the sphere material, the less time the infusion requires.

Formally, integrating (23) produces:

$$\tau(\lambda)=\int_{\lambda}^{\lambda_{init}}\frac{x^9}{\left[\left(x^6-1\right)\left(\frac{J_{\max}}{J_{\max}-J(x)}\right)-\tilde{P}_{sphyg}x^7\right]}dx \tag{25}$$

where $\lambda_{init}\left[\geq \lambda\right]$ is the initial stretch ratio, which is determined by the amount of analgesic to be infused. The structure of the elastomeric sphere requires that $\lambda \geq 1$.

Solving Equation (16) for the function $\tilde{Q}(\lambda)$ and Equation (25) for the function $\tau(\lambda)$ gives us a parametric description of the normalized volumetric flux $\tilde{Q}$ as a function of normalized time τ, that is, $\tilde{Q}(\tau)$. Figure 2 illustrates this functional dependence. The curve in Figure 2 is shape-wise close to those observed in Figure 3C and Figure 3D of Reference [5].

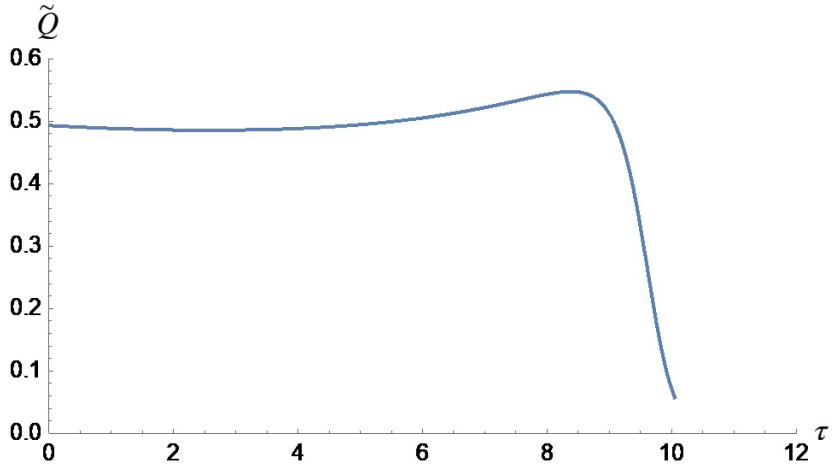

Figure 2. Normalized flux $\tilde{Q}$ versus normalized time τ from (16) and (25) given the parameters $\lambda_{\max} = 4$, $\lambda_{init} = 2.5$, and $\tilde{P}_{sphyg} = 0.1$. Note that these parameters are the same as those used in the caption of Figure 1.

6. Self-Consistency Conditions

We now review the conditions under which quasi-static, Poiseuille flow obtains. There are three related, but distinct, conditions: 1) the time required to establish Poiseuille flow $\rho R^2/\mu\lambda_B^2$ is much shorter than the time for the spherical reservoir to drain T; 2) the distance or "entrance length" $\left(\rho R^2/\mu\lambda_B^2\right)\bar{u}$ over which Poiseuille flow is established in the tube connecting the pump with the port is much shorter than the length of the tube L; and 3) the Reynolds number Re of the flow in the cylindrical tube is smaller than the number 2300 at which the flow becomes turbulent.

These three conditions are:

$$\frac{\rho R^2}{\mu\lambda_B^2} \ll T, \tag{26a}$$

$$\left(\frac{\rho R^2}{\mu\lambda_B^2}\right)\bar{u} = L, \tag{26b}$$

and

$$Re\left[=\frac{\rho R}{\mu}\bar{u}\right] \ll 2300. \tag{26c}$$

where, $\lambda_B \left[\approx 2.40\right]$ is the first root of the zeroth order Bessel function. See References [8] or [10]. The average fluid speed in the tube $\overline{u}\left[=V/\pi R^2 T\right]$ is defined in terms of the drain time T, the fluid flux $\pi R^2 \overline{u}$, and the volume V in the filled sphere $V=\left[4\pi r_{init}^3\left(\lambda_{init}^3-1\right)/3\right]$, so that $\pi R^2\overline{u}=4\pi r_{init}^3\left(\lambda_{init}^3-1\right)/3T$. The parameters describing a typical elastomeric pump and the physical properties of the fluid necessary to test these inequalities are collected in **Table 1**. For this purpose, we have assigned a drain time T of one hour (3600 seconds). Most infusion times are longer. But the shorter T, the less well observed the inequalities (26). All units are SI.

Table 1. Parameters typical of an elastomeric pump [14] used in computing the inequalities (27) from (26).

R	r_{init}	λ_{init}	μ	ρ	T	L
radius of tube	initial radius of spherical pump	initial stretch ratio	viscosity of fluid	density of fluid	infusion time	length of tube
0.002	0.02	2.5	0.001	1000	3600	0.5

These values transform inequalities (26) respectively into:

$$0.69 \ll 3600\,, \tag{27a}$$

$$0.0075 \ll 0.5\,, \tag{27b}$$

and

$$22 \ll 2300\,. \tag{27c}$$

Although not all elastomeric pumps will be described by the values in **Table 1**, the most variation will be in the infusion time T, which instead of 1 hour could be as long as 24 or 48 hours. These longer times will make the inequalities (26) and (27) even stronger. As a result, the flow within the tube of the elastomeric tube is laminar, quasistatic, and Poiseuille.

7. Beyond Poiseuille

If the conditions for laminar, Poiseuille flow are not justified, one may use the Darcy-Weisbach equation [15]. In this case, the pressure drop ΔP along a pipe is:

$$\frac{\Delta P}{L}=f\frac{\rho\overline{u}^2}{4R}\,. \tag{28}$$

where, f is the friction factor for which Blasius's formula is [16]:

$$f=\frac{K}{Re^{1/4}} \tag{29}$$

with $K=0.3164$. Combining (28) and (29) and the definition of the Reynolds number, in this geometry, $Re=\rho R\overline{u}/\mu$, produces:

$$\frac{\Delta P}{L}=K\frac{\rho^{5/4}\overline{u}^{7/4}}{4R^{3/4}\mu^{1/4}}\,. \tag{30}$$

Since the volumetric flux $Q=\pi R^2\overline{u}$, we find that:

$$Q = \frac{\pi R^2}{L}\left(\frac{4R^{3/4}\mu^{1/4}}{\rho^{5/4}K}\right)^{4/7}\left(P_{elast} - P_{sphyg}\right). \tag{31}$$

As before, this flux is due to the pressure drop from the elastomeric pump. Therefore,

$$Q = \frac{2wE\pi R^2}{3r_{\min}L}\left(\frac{4R^{3/4}\mu^{1/4}}{\rho^{5/4}K}\right)^{4/7}\left[\left(\frac{1}{\lambda}\right)\left(1-\frac{1}{\lambda^6}\right)\left(\frac{1}{1-\dfrac{J(\lambda)}{J(J_{\max})}}\right) - \tilde{P}_{sphyg}\right]. \tag{32}$$

In this case, we end up with the same functional relationship for Q as before, but with different normalizing constants. For other approximations to the friction factor, such as the Colebrook-White equation, numerical solutions are required.

A further generalization is to non-Newtonian fluids [17]. The pipe flow rate of a power-law fluid is:

$$Q = \frac{\pi n R^3}{3n+1}\left(\frac{R\Delta P}{2\mu L}\right)^{1/n}, \tag{33}$$

where n is the power-law index of the specific fluid under consideration. This gives rise to a simple extension of the Newtonian case, as it leads to the dimensionless evolution Equations (16) and (23) albeit with different definitions of the dimensionless time and pressure.

Studies in organ perfusion show that, in this case, ordinary Poiseuille flow is not an appropriate model. After all, the difference in flows between Marshall's hyperosmolar and "University of Wisconsin" solutions do not follow the Newtonian formulation of Poiseuille flow [18]. As reverse flow—from a blood vessel at relatively high pressure to an inflatable sphere at zero pressure—could be considered a mathematical model for blood donations, this power-law model might work well, given the non-Newtonian behavior of blood [19].

For both Darcy-Weisbach and power-law fluids, the stretch ratio λ at peak toxicity is $7^{1/6}$.

8. Discussion

We have obtained, in (16), an analytic expression for the dimensionless flow rate $\tilde{Q}(\lambda)$ in terms of the stretch ratio $\lambda\left[=r/r_{\min}\right]$ of the elastomeric sphere. A solution whose characterizing parameters are representative of empirical studies is plotted in **Figure 1**. This same solution is presented as a normalized time-dependent function $\tilde{Q}(\tau)$, as defined by the parametric Equations (16) and (25), in **Figure 2**.

Increasing the elastomer's maximum possible stretch from $\lambda_{\max} = 4$ to $\lambda_{\max} = 6$ increases the relative size of the toxicity bump, as shown in **Figure 3**, which illustrates the problem with making $\lambda_{\max}$ it too large. On the other hand, the toxicity bump may be minimized by inflating the elastomeric ball more closely to the limit $\lambda_{\max} = 4$, as shown in **Figure 2**.

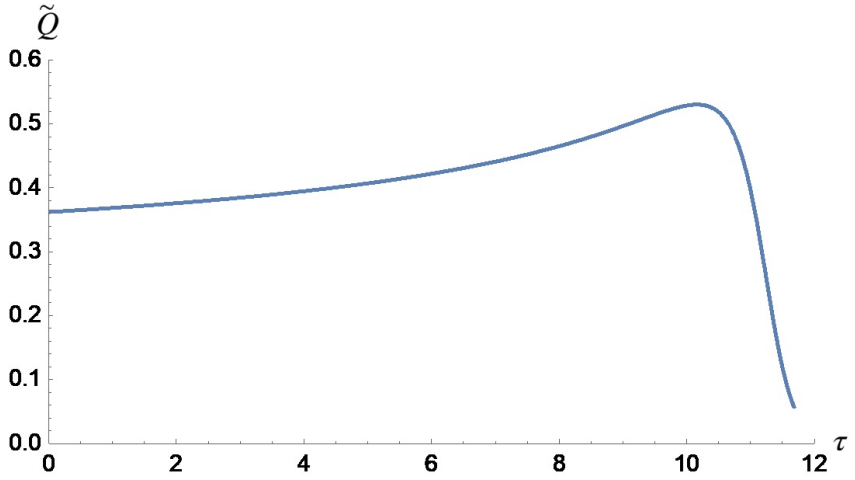

Figure 3. Normalized flux $\tilde{Q}(\tau)$ from (16) and (25) given the parameters $\lambda_{\max} = 6$, $\lambda_{init} = 2.5$, and $\tilde{P}_{sphyg} = 0.1$. Note the difference from **Figure 2**.

The values characterizing **Figure 1** and **Figure 2**, $\lambda_{init}\left[\approx 2.5\right]$ and $\lambda_{\max}\left[\approx 4.0\right]$, are close to optimal for limiting the toxicity bump to less than 10% of the constant value. Furthermore, $\lambda_{\max} \gg \lambda_{peak}\left[=1.38\right]$ is necessary to produce an infusion time with a relatively long, constant period followed by a rapid termination.

These model results are in broad agreement with the curves determined experimentally. That is, to say, the initial flow rate is relatively constant, rises gently over time, and reaches a peak flow rate just before it drops sharply as the infusion ends. The dependence of the infusion time on the elastic properties of the elastomeric pump also supports observations [20] [21] that refilling such a pump can significantly affect the flow rates, given potential hysteresis effects on the elastomeric ball.

We have shown that the time taken for a sphere of antibiotic fluid to infuse into a patient becomes longer when the fluid has a higher viscosity; the catheter line is lengthened (which decreases the pressure gradient for a given pressure drop); the elastic constant of the sphere is decreased, so it exerts less pressure on the fluid; the radius of the catheter is decreased; the initial radius of the elastic sphere is decreased; and when the pressure in the blood vessel is increased. These theoretical results match those found experimentally by Hodge and Fleischer [22] and others [23].

9. Conclusions

In this paper, we propose a quasi-static model for laminar flow from the elastic sphere of an elastomeric pump into a tube delivering analgesics or other medicines to a blood vessel. Our model of the elastomeric spherical reservoir exploits Gent's equation of state for elastic spheres and leads to a flow in the tube connecting the pump and the catheter that is both quasi-static and Poiseuille. The theoretical prediction of the flow rate closely matches the pattern in laboratory experiments. We predict the stretch ratio at which the peak flow rate, the "toxicity bump",

occurs near the end of infusion. Consequently, one can design pumps that minimize this bump.

The infused fluid, volume flux as a function of time, also closely follows previous experimental results as it is approximately constant in time, followed by a toxicity bump, and then drops sharply as the infusion time is approached.

We also developed other model equations by combining the Darcy-Weisbach flow and the Blasius friction factor for rapid fluid flows, such as in the infusion of therapeutic agents in emergency situations.

The quasi-static approximation developed here could also be of wide use in modeling other physiological fluid flows [24]. It can be of advantage, for example, when a viscous flow is clearly no longer time independent and for which Bernoulli flow would not be an appropriate description [25]. In addition, it complements other methods used in biological fluid mechanics, such as pulsed flow equations [26] or peristaltic models for blood flow in stenosed arteries [27].

Further research could generalize and further specify the model by adding friction to the tube-fluid interaction via a Darcy-Weisbach pressure drop and by developing non-Newtonian and power-law models of the infusion fluid.

In conclusion, the authors develop a theoretical model that can be used to design and optimize elastomeric pumps, which allow patient mobility, for the infusion of analgesics and antibiotics.

Conflicts of Interest

The authors declare no conflicts of interest regarding the publication of this paper.

References

[1] Healy, D.P., Sahai, J.V., Fuller, S.H. and Polk, R.E. (1990) Vancomycin-Induced Histamine Release and "Red Man Syndrome": Comparison of 1- and 2-Hour Infusions. *Antimicrobial Agents and Chemotherapy*, **34**, 550-554. https://doi.org/10.1128/aac.34.4.550

[2] Sivagnanam, S. and Deleu, D. (2003) Red Man Syndrome. *Critical Care*, **7**, Article No. 119. https://doi.org/10.1186/cc1871

[3] Murthy, V., Wilson, J., Suhr, J., James, L., Tombs, H., Shereef, E., *et al*. (2019) Moving Cancer Care Closer to Home: A Single-Centre Experience of Home Chemotherapy Administration for Patients with Myelodysplastic Syndrome. *ESMO Open*, **4**, e000434. https://doi.org/10.1136/esmoopen-2018-000434

[4] Barton, A., Fisher, E. and Rees-Milton, M. (2023) Elastomeric, Fillable Infusion Pumps: An Overview for Clinical Practice. *British Journal of Nursing*, **32**, 3-7. https://doi.org/10.12968/bjon.2023.32.sup15.3

[5] Remerand, F., Vuitton, A.S., Palud, M., Buchet, S., Pourrat, X., Baud, A., *et al*. (2008) Elastomeric Pump Reliability in Postoperative Regional Anesthesia: A Survey of 430 Consecutive Devices. *Anesthesia & Analgesia*, **107**, 2079-2084. https://doi.org/10.1213/ane.0b013e318187c9bb

[6] Weisman, R.S., Missair, A., Pham, P., Gutierrez, J.F. and Gebhard, R.E. (2014) Accuracy and Consistency of Modern Elastomeric Pumps. *Regional Anesthesia and Pain Medicine*, **39**, 423-428. https://doi.org/10.1097/aap.0000000000000130

[7] Gent, A.N. (2005) Elastic Instabilities in Rubber. *International Journal of Non-Linear Mechanics*, **40**, 165-175. https://doi.org/10.1016/j.ijnonlinmec.2004.05.006

[8] Batchelor, G.K. (1967) An Introduction to Fluid Dynamics. Cambridge University Press.

[9] Wadhwa, Y.D. and Wineinger, T.W. (1968) Linear Time-Dependent Fluid Flow Problems. *Quarterly of Applied Mathematics*, **26**, 1-9. https://doi.org/10.1090/qam/99870

[10] Landau, L.D. and Lifshitz, E.M. (1987) Course of Theoretical Physics, Vol. 6: Fluid Mechanics. 2nd Edition, Pergamon Press, 53-54.

[11] Lemons, D.S., Lipsombe, T.C. and Faehl, R.J. (2022) Vertical Quasistatic Poiseuille Flow: Theory and Experiment. *American Journal of Physics*, **90**, 59-63. https://doi.org/10.1119/10.0006245

[12] Merritt, D.R. and Weinhaus, F. (1978) The Pressure Curve for a Rubber Balloon. *American Journal of Physics*, **46**, 976-977. https://doi.org/10.1119/1.11486

[13] Guiffant, G., Durussel, J., *et al*. (2011) Mechanical Performances of Elastomers Used in Diffusers. *Medical Devices*: *Evidence and Research*, **2011**, 71-76. https://doi.org/10.2147/mder.s18633

[14] Braun, B. (2024) Elastomeric Pump Systems for Short-Term and Long-Term Infusions Brochure. https://www.bbraunusa.com/en/products/b4/easypump-st-lt.html

[15] Darcy, H. (1857) Recherches expérimentales relatives au mouvement de l'eau dans les tuyaux. Vol. 1, Mallet-Bachelier.

[16] Blasius, H. (1913) Das Aehnlichkeitsgesetz bei Reibungsvorgängen in Flüssigkeiten. In: Ingenieure, V.d., Ed., *Mitteilungen über Forschungsarbeiten auf dem Gebiete des Ingenieurwesens*, Springer, 1-41. https://doi.org/10.1007/978-3-662-02239-9_1

[17] Akram, J. and Akbar, N.S. (2020) Biological Analysis of Carreau Nanofluid in an Endoscope with Variable Viscosity. *Physica Scripta*, **95**, Article ID: 055201. https://doi.org/10.1088/1402-4896/ab74d7

[18] Singh, S., Randle, L.V., Callaghan, P.T., Watson, C.J.E. and Callaghan, C.J. (2013) Beyond Poiseuille: Preservation Fluid Flow in an Experimental Model. *Journal of Transplantation*, **2013**, 1-6. https://doi.org/10.1155/2013/605326

[19] Lee, S.H., Han, K., Hur, N., Cho, Y.I. and Jeong, S. (2019) The Effect of Patient-Specific Non-Newtonian Blood Viscosity on Arterial Hemodynamics Predictions. *Journal of Mechanics in Medicine and Biology*, **19**, Article ID: 1940054. https://doi.org/10.1142/s0219519419400542

[20] Mohseni, M. and Ebneshahidi, A. (2014) The Flow Rate Accuracy of Elastomeric Infusion Pumps after Repeated Filling. *Anesthesiology and Pain Medicine*, **14**, e14989. https://doi.org/10.5812/aapm.14989

[21] Grant, C.R.K. and Fredrickson, M.J. (2009) Regional Anaesthesia Elastomeric Pump Performance after a Single Use and Subsequent Refill: A Laboratory Study. *Anaesthesia*, **64**, 770-775. https://doi.org/10.1111/j.1365-2044.2009.05941.x

[22] Hodge, D. and Fleisher, G. (1985) Pediatric Catheter Flow Rates. *The American Journal of Emergency Medicine*, **3**, 403-407. https://doi.org/10.1016/0735-6757(85)90198-6

[23] Berman, D.J., Schiavi, A., Frank, S.M., Duarte, S., Schwengel, D.A. and Miller, C.R. (2020) Factors That Influence Flow through Intravascular Catheters: The Clinical Relevance of Poiseuille's Law. *Transfusion*, **60**, 1410-1417. https://doi.org/10.1111/trf.15898

[24] Winston, B.A., VanSickle, D. and Winston, K.R. (2016) Resistance to Venous Flow.

Journal of Trauma and Acute Care Surgery, **81**, 333-338. https://doi.org/10.1097/ta.0000000000001077

[25] Uno, Y. (2018) Colonic Transit Time and Pressure Based on Bernoulli's Principle. *Clinical and Experimental Gastroenterology*, **11**, 153-163. https://doi.org/10.2147/ceg.s153676

[26] San, O. and Staples, A.E. (2012) An Improved Model for Reduced-Order Physiological Fluid Flows. *Journal of Mechanics in Medicine and Biology*, **12**, Article ID: 1250052. https://doi.org/10.1142/s0219519411004666

[27] Misra, J.C., Sinha, A. and Shit, G.C. (2008) Theoretical Analysis of Blood Flow through an Arterial Segment Having Multiple Stenoses. *Journal of Mechanics in Medicine and Biology*, **8**, 265-279. https://doi.org/10.1142/s0219519408002620